

Experimental Study of 2D-Instabilities of Hydrogen Flames in Flat Layers

M. Kuznetsov^{1*}, J. Grune², S. Tengah¹, J. Yanez¹

¹Institute for Energy and Nuclear Energy, Karlsruhe Institute of Technology,
Hermann-von-Helmholtz Platz 1, 76344, Eggenstein-Leopoldshafen, Germany

²Pro-Science GmbH, Parkstrasse 9, 76275, Ettlingen, Germany

1 Introduction

Many researchers have performed experiments and numerical simulations of hydrogen flame behavior and instabilities in one-dimensional geometries such as a tube or a three-dimensional geometry similar to a spherical bomb chamber. Therefore, there is limited knowledge on how hydrogen flame behaves in two-dimensional geometries. One-dimensional geometries have the advantage of being simple to investigate. However, the presence of boundary layer effects are inevitable in this kind of configuration. While three-dimensional geometry has no boundary layer issues to be considered and is similar in the real scenario, it is very complex to experimentally interpret the effect of flame instabilities on the hydrogen flame propagation. Experimental investigations of hydrogen flames in two-dimensional geometries have the advantage that the boundary layer effect is reduced and the structure of the flame instability in a radial direction will be developed and clearly distinguished.

The main purpose of the current work was to experimentally investigate the effect of instabilities on the hydrogen flame behavior in a planar two-dimensional geometry. The main interest of this work was to investigate how instability affects the flame propagation and whether flame acceleration would occur in such configurations leading to the transition from deflagration to detonation (DDT). The results of this work can later be used for theoretical analysis of flame acceleration and DDT phenomena as well as for numerical code validation

2 Experimental Details

The experimental investigation in the present work was performed for H_2 – air and H_2 – O_2 mixtures in between a transparent glass plate assembly with a constant volume. Figure 1 shows the complete view of the facility. The experimental facility consists of the glass plate assembly (a), fuel and oxidizer intake and exhaust system, an ignition system (b), an optical schlieren system combined with a high speed camera, data acquisition and control system.

The glass plate assembly (Fig. 1, (a)) is made up of two transparent Quartz/Plexiglas plates with spacers placed in between to create parallel gaps of 2, 4 and 6 mm. Experiments are carried out in a squared frame with dimensions of 500 x 500 mm. The optical access system limits the observable view to a light beam view of 300 x 300 mm. The mixture within the glass plate assembly was ignited in the center using a spark electrode igniter (Fig. 1, (b)).

Flame propagation was visualized and investigated optically using a schlieren method combined with high-speed photography. The schlieren method enables the visualization of density gradients due to the combustion process, even in optically transparent media.

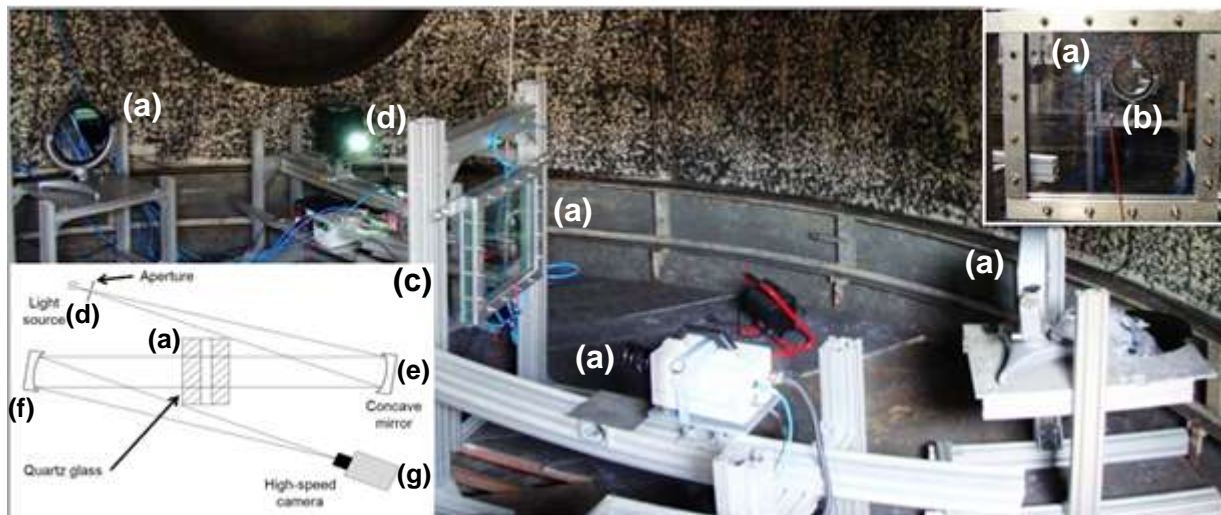


Figure 1. Side view of experimental facility

The shadowgraph system implemented in this work is a standard schlieren Z-configuration system and is shown as a sub-image (c) in Figure 1. A halogen lamp (d) was used as a light source. The light passes through an aperture and is reflected by the first concave mirror (e). When the parallel light rays enter the assembly (a) and hit the flame front, they get refracted or bent out of their original paths. These refracted light rays get reflected by the second concave mirror (f) towards the high-speed camera (g), which records the shadow images of the whole combustion process. The high-speed camera (Fastcam SA1.1, Photron) records the schlieren image combustion process.

Flame propagation of hydrogen combustion was investigated for H_2 – air and H_2 – O_2 mixtures. Hydrogen-air mixtures in the range 7-60% H_2 and hydrogen-oxygen mixtures from 13 to 80% H_2 were tested in the current work. Mass flow rate controllers were used to inject premixed composition directly into the gap. The test mixture was injected from the top by replacing air through the bottom outlet lines until the exhausted gas becomes the same as the injected composition. The mixture was isolated by a plastic foil around the peripheral sides, initially open to the atmosphere. The foil was lightly fixed around the gas periphery to provide a weak opening after ignition and homogenous combustion process. All experiments were performed at ambient conditions of 1 bar and 293 K.

3 Experimental Results and Analysis

Flame propagation of the hydrogen combustion recorded by the high-speed camera was analyzed by using an image processing tool *ImageJ*. The reference scale image taken at the beginning of an experimental series is then used to convert pixels into meters. Figure 2 shows an example of flame propagation for a very lean mixture of 10% H_2 in air. The thermo-diffusion and Landau- Darrieus instabilities lead to the development of a double-mode cellular structure of the flame surface. The primary thermo-diffusion instability appears almost immediately after the ignition, leading to quite uniform, relatively small-size mode of cellular structure. Then, the large-size mode of cellular structure due to Landau- Darrieus instability develops with a growing cell size similar to the flower petals. Since the Markstein number becomes positive for hydrogen-air mixtures above 15% H_2 it changes the sensitivity of the flame to thermo-diffusion instability. In Fig. 3 a very smooth flame surface may be seen for mixtures with 30 and 50% H_2 in air at the initial stage of the process. After a flame radius of the order of 10-15 cm, the cellularity of the flame surface appears due to Landau- Darrieus instability.

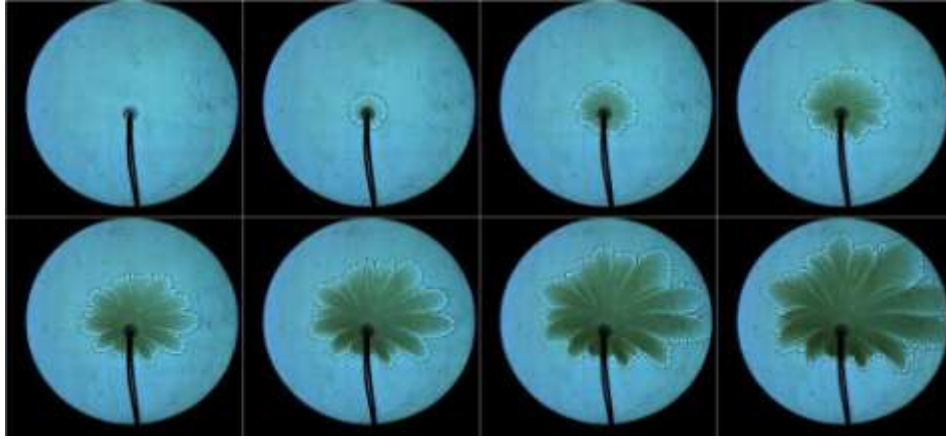


Figure 2. Flame propagation of lean H_2 – air mixture for 10% H_2 in air in a 6-mm gap layer.

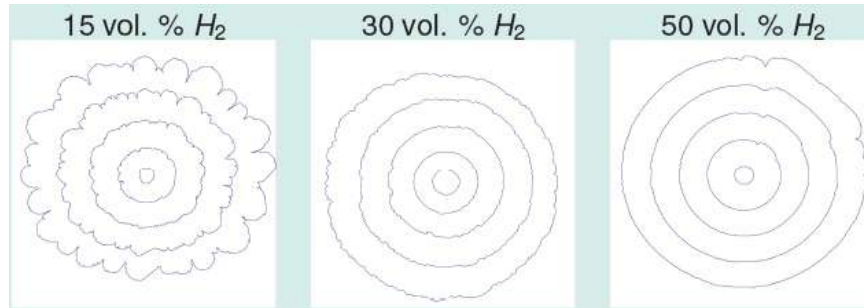


Figure 3. Flame propagation of lean H_2 – air mixture for 15, 30 and 50% H_2 in air in a 6-mm gap layer.

Since the combustion process in our facility takes place at ambient pressure and temperature, the advantage of such an experimental layout that directly measures the flame radius can be used to evaluate the laminar flame velocity. The flame front velocity was calculated by taking the difference between the instantaneous radius of the flame front, r_f and igniter position, r_0 divided by the actual time difference.

When the combustible mixture is ignited, the ignition energy influences the velocity of the flame propagation, resulting in a very high flame velocity. From the obtained velocity measurement, it can be observed that the flame starts to propagate free of ignition influences at around $r_f \sim 0.03$ m. Therefore, only flame velocities of $r_f > 0.03$ m are taken into consideration in this work (Fig. 4). The stretch-free laminar burning velocity were obtained by linear extrapolation of a plot of the laminar burning velocity S_L as a function of the stretch rate K (Fig. 5). The laminar burning velocity S_L is first calculated by dividing the flame front velocity S_F by the expansion factor σ and stretch rate K . Assuming a linear correlation, the influence of the flame front stretch on the laminar flame speed can be specified by Markstein length L_M :

$$S_L(K) = S_{L,s} - L_M \cdot K \quad (1)$$

where $S_L = S_F/\sigma$, and $S_{L,s}$ are the stretched and free of stretch laminar flame velocities, A is the visible flame area for flame radius r_f and a layer thickness h , $A = 2\pi r_f h$, K is the stretch rate calculated for planar 2D case as follows

$$K = \frac{1}{A} \frac{dA}{dt} = \frac{1}{r_f} \frac{dr_f}{dt} \quad (2)$$

The stretch rate in a planar geometry (Eq. 2), is two times smaller compared to a spherical geometry. The linear extrapolation of the curve (Fig. 5) was determined by using the least square fit method and

the stretch-free laminar burning velocity $S_{L,s}$ is simply the y-intercept of the line fit, whereas the slope of the line gives the Markstein length, L_m .

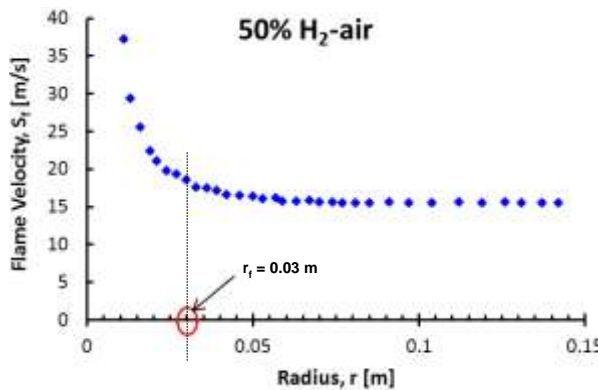


Figure 4. Flame velocity plotted against flame radius (50% H_2 in H_2 – air mixture).

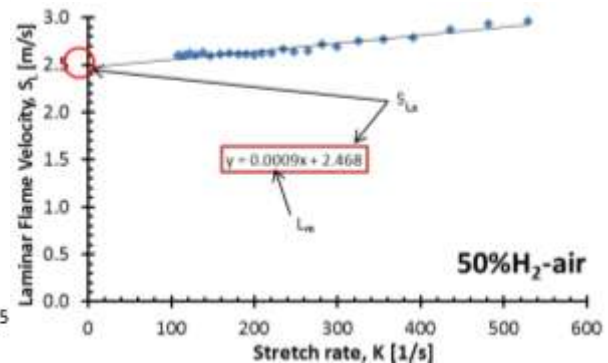


Figure 5. Laminar burning velocity plotted as a function of stretch rate (50% H_2 in H_2 – air mixture)

Through the optical measurement, the influence of the stretch effect on the flame, characterized by Markstein length L_m , was obtained. Figure 6 shows the relationship between laminar burning velocity S_L and the stretch rate K over different stoichiometry of H_2 – air mixtures for a peripherally open configuration with central ignition at gap size 6 mm. The Markstein length characterizes the stability of hydrogen flames against the thermal diffusive instability. Unstable thermal-diffusive flames have $L_m < 0$, while stable thermal-diffusive flames have $L_m > 0$. A negative sign of the Markstein length means stretch effect causes an acceleration of the curved flame, whereas a positive sign means the stretch effect causes a deceleration of the curved flame. Figure 7 shows that the sign of the Markstein length varies from negative to positive as the concentration of H_2 increases. Lean premixed H_2 – air mixtures ($<15\% H_2$) have a negative sign and the burning velocity of the lean mixtures increases with increasing stretch rate, resulting in an acceleration of the flame front. Lean mixtures above 15% H_2 , stoichiometric and rich mixtures have a positive sign and the burning velocity is observed to decrease with increasing stretch rate, resulting in the deceleration of the flame front. This decelerating behavior of the flame front is also observed for all investigated H_2 – O_2 mixtures. The Markstein length for the range of concentration of H_2 - O_2 mixtures investigated in this work were found to be positive for all concentrations, verifying that H_2 – O_2 flames are stable against thermal diffusive instability.

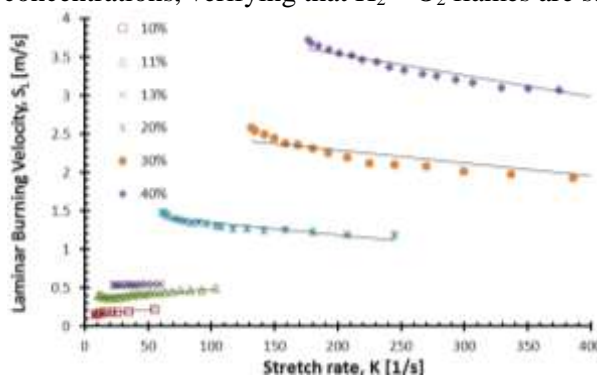


Figure 6. Laminar burning velocity as a function of stretch rate K for H_2 – air mixtures

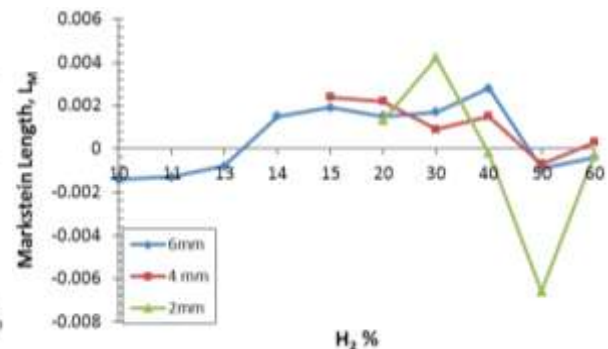


Figure 7. Markstein length in dependency of H_2 concentration for H_2 – air mixtures

Despite being stable against thermal-diffusive instability, the cellular structure still develops in stoichiometric and rich premixed H_2 -air flames. This can be attributed to hydrodynamic Landau-Darrieus instability, which is an intrinsic property in all premixed flames. The tested premixed H_2 – O_2

mixtures have $Le > 1$ and hence, are stable against thermal-diffusive instability. The cellular structure observed for these mixtures is only attributable to the hydrodynamic instability.

For lean H_2 – air mixtures, the flame initially propagates with a smooth surface but very quickly starts to form bulbs as the flame reaches a critical radius. As the flame continues to expand, these bulbs multiply, resulting in a cellular structure of the flame surface. The cellular structure continues to develop as the flame propagates outwards. For instance, the image post-processing performed for 15% hydrogen-air mixture shows a dynamic of flame wrinkling against time for different directions in 2D and 3D plots (Fig. 8). For rich H_2 – air mixture, the flame propagates with a very symmetrical and smooth surface. The surface becomes wrinkled at later stage of the flame propagation i.e. at a larger radius compared to the lean mixtures. The wrinkling surface then further develops into a cellular structure as well. The cellular development pattern observed for H_2 – air is analogous for flame propagation in H_2 – O_2 . The only significant difference is that H_2 – O_2 flames propagate at a much faster rate than H_2 – air flames. Since the flame velocity is proportional to the flame area the wrinkled surface leads to flame velocity amplification factor $\Xi = 1.2-1.5$, similar to that obtained in our theoretical analysis [1] based on the derivation of the Sivashinsky equation [2].

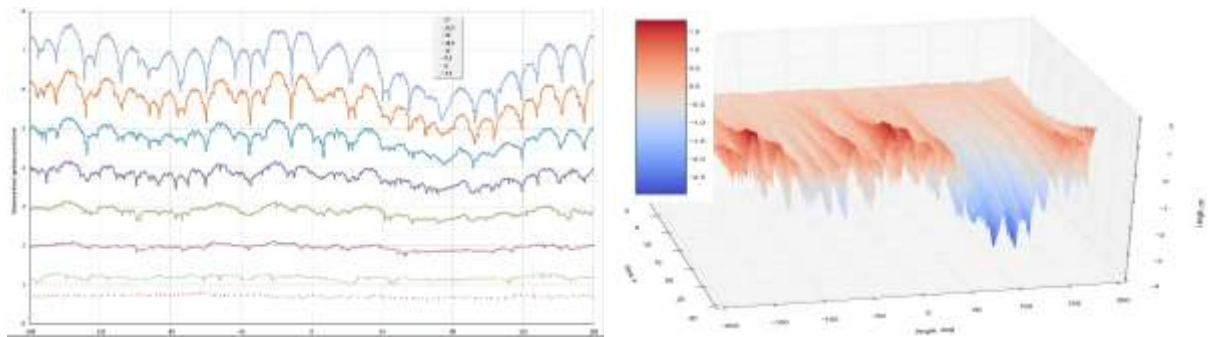


Figure 8. Dynamics of flame instability for 15% H_2 in air in 2D (left) and 3D (right) plots vs. direction (from -180° to $+180^\circ$). Each line in 2D plot corresponds to 3.5, 6, 9.5, 13, 16.5, 20, 23.5 and 27 s after ignition. Right scale in 3D plot corresponds to deepness of the funnels (from -4 to $+2$ cm) relatively the average flame position.

Through optical measurement, the stretch-free laminar burning velocity of the hydrogen flame can be obtained. The laminar burning velocity strongly depends on the H_2 concentration and gap size. These dependencies can be seen in Figure 9 and 10 for H_2 – air and H_2 – O_2 . In general, the laminar burning velocity at lean composition (for H_2 – air: $H_2\% < 30\%$, for H_2 – O_2 : $H_2\% < 66.6\%$) increases with increasing H_2 concentration, reaching its maximum between 30% and 40% for H_2 – air mixture, and between 60% and 66.6% for H_2 – O_2 mixture. As the mixture gets richer, the velocity starts decreasing.

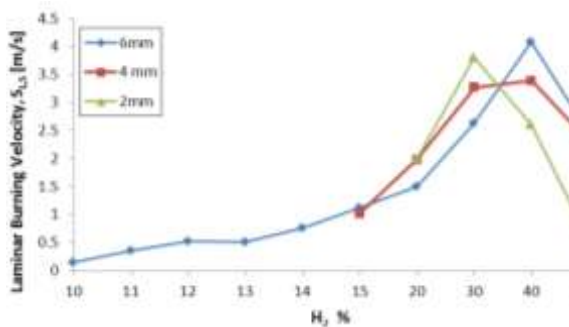


Figure 9. Stretch-free laminar burning velocity vs. H_2 concentration at different gap sizes for H_2 – air

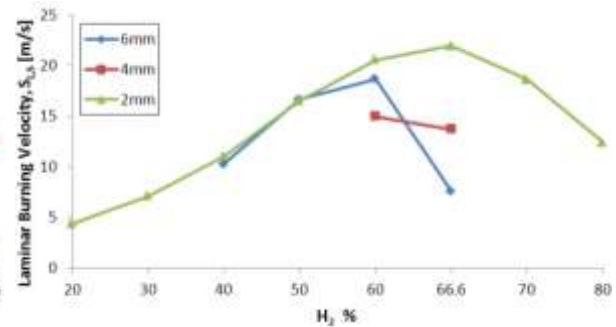


Figure 10. Stretch-free laminar burning velocity vs. H_2 concentration at different gap sizes for H_2 – O_2

When decreasing the gap size, the stretch-free laminar burning velocity is observed to increase on the lean side of H_2 – air mixture but decreases on the rich side of the mixture as H_2 concentration

increases. The behavior on the rich side is attributable to the high thermal conductivity of hydrogen. As the gap size decreases, the surface area-to-volume ratio increases. This results in higher heat loss as the mixture gets richer, which causes the velocity to decrease. On the lean side of the mixture, the heat loss is not as high as in the rich mixture. The flame dynamics is now governed by the geometry factor or increasing flame area. As the gap size decreases, the specific area of the flame gets higher, causing the burning velocity to increase for 2D-geometry as follows

$$S_f = \frac{dx}{dt} = \frac{A}{A_0} \sigma S_L = \frac{2\pi x(x+h)}{2\pi xh} \sigma S_L = \left(1 + \frac{x}{h}\right) \sigma S_L \quad (3)$$

where $A=2\pi x^2$ is the visible flame area which is proportional to the flame radius x in a layer with a constant gap h ; A_0 is the initial flame area assumed to be ring-shaped $A_0=2\pi xh$; $\sigma=\rho_u/\rho_b$ is the expansion ratio of combustion products compared to the unreacted mixture; S_L is the fundamental laminar flame speed. This means that as for “finger flames” in a planar 2D geometry, the visible flame velocity is inversely proportional to the gap size h so that that when approaching an infinite layer thickness ($h \rightarrow \infty$) the flame velocity should also approach to the laminar flame speed for a planar flame. The theoretical planar laminar burning velocity for stoichiometric H_2 – air is 2.30 m/s. The extrapolated laminar velocity obtained for the same mixture is 2.25 m/s, indicating that the result obtained is in good agreement with the theoretical values and the method can be used for laminar flame velocity evaluation taking into account stretch effect and a gap size.

4 Conclusions

Hydrogen flame behavior in two-dimensional geometry was experimentally investigated. Hydrogen combustion of H_2 – air and H_2 – O_2 mixtures were carried out within the gap of two transparent quartz plates spaced by 2, 4 and 6 mm.

Flame propagation within the glass plate assembly was visualized using the shadowgraph method. To analyze the influence of flame instabilities, the stretch-free laminar burning velocity of the flame and Markstein length were determined via post-processing of optical measurement. Negative Markstein lengths were obtained for lean H_2 – air mixtures ($< 14\% H_2$). The results also show that the laminar burning velocity strongly depends on H_2 concentration and gap size.

The appearance of the cellular structure for H_2 – air mixtures was found as a result of two main intrinsic instabilities of the flame, thermal – diffusive instability and hydrodynamic instability, namely Landau – Darrieus instability. Wrinkling of the flame due to the flame instability and enhanced flame area result in a flame velocity amplification factor $\Xi = 1.2-1.5$, which is the same as found by derivation of the Sivashinsky equation [1, 2].

Within the scale of this work, significant flame acceleration and DDT phenomena were not observed. Beyond the frames of current work the DDT phenomena was only observed for stoichiometric hydrogen-oxygen mixtures in between two plates of 1x1 m with a gap size of 2 mm [3]. Characteristic run-up-distance to DDT was found to be of the order of 20 cm from the ignition point.

References

- [1] Yanez J, Kuznetsov M. (2015). An analysis of flame instabilities based on Sivashinsky equation. Submitted to 25 ICDERS.
- [2] Sivashinsky G. (1977). Nonlinear analysis of hydrodynamic in laminar flames. I. Derivation of basic equations, *Acta astronautica*, 4: 1177–1206.
- [3] Kuznetsov M., Kinetic and Gasdynamic Aspects of DDT in Different Geometries, *Proc. of the Thirty-Fifth International Symposium on Combustion*, San Francisco, CA, USA, 3–8 August 2014, paper WP2P124